Proceedings of IMECE2006
2006 ASME International Mechanical Engineering Congress and Exposition
November 5-10, 2006, Chicago, Illinois, USA

IMECE2006-14311

A MULTIVARIABLE APPROACH TO EGR-VGT ACTUATOR CONTROL PROBLEM

Shreekant Gayaka
Ray W. Herrick Labs
School of Mechanical Engineering
Purdue University
West Lafayette, Indiana 47907
Email: sgayaka@purdue.edu

Bin Yao
School of Mechanical Engineering
Purdue University
West Lafayette, Indiana 47907
Email: byao@purdue.edu

Peter H. Meckl
School of Mechanical Engineering
Purdue University
West Lafayette, Indiana 47907
Email: meckl@purdue.edu

ABSTRACT

The combined use of Variable Geometry Turbine (VGT) and Exhaust Gas Recirculation (EGR) gives us an opportunity to reduce emissions, without compromising the need to generate more power. In the present work, a multivariable approach is used to tackle the EGR-VGT actuator control problem. A linear multivariable controller is designed using Lyapunov's Indirect Method, based on the Jacobian matrix of the system. Then, some stronger conditions are sought to be satisfied by the Jacobian matrix, which would ensure the Global Asymptotic Stability of the system. These conditions are derived using Nonlinear Contraction Analysis. Finally, simulations are performed on a simplified model with three states to evaluate the performance of the controllers.

1 Introduction

Diesel engines are among the most efficient internal combustion engines [1]. Among the key factors that are limiting the use of diesel engines at the moment are: (a) relatively low power output and, (b) high content of unwanted oxides, hydro-carbons and particulate matter in the exhaust (see [2] and [3]). The power output can be increased by increasing the boost pressure, which is accomplished by using a turbocharger. However, with more stringent emissions regulations, the problem of exhaust gas purification persists. A possible solution to this critical problem is to use an Exhaust Gas Recirculation (EGR) scheme in conjunction with Variable Geometry Turbine (VGT). Such a combination gives us more flexibility in controlling the system. But, it must also be mentioned that the EGR-VGT interactions significantly affect the system dynamics and decoupling their effects for design purposes will seriously compromise the performance of the controller. Hence, the resulting nonlinear multivariable system calls for more sophisticated control strategies that allow us to take full advantage of the added flexibility in controlling the system. The ever-increasing complexity of Electronic Control Units (ECU) can provide us with the necessary resources to implement such advanced control algorithms.

In the present work, we use a simplified 3-state plant for the purpose of controller design. In the next section, we briefly describe the diesel engine model and the underlying assumptions. In the third section, we formulate the basic control problem and explain two strategies that have been used for controller design. First, a linear multivariable controller is designed using the plant model, linearized about the equilibrium point . A linear controller is simpler to implement and this method shows the effectiveness of a linear controller in solving this nonlinear control problem.And second, a nonlinear multivariable controller is designed based on Nonlinear Contraction Analysis, which is an extension of the Krasovskii's theorem [4]. This method also serves the purpose of illustrating how Nonlinear Contraction Analysis can be used for the purpose controller design. Conclusions and simulation results are presented in the final section.

2 The Diesel Engine Model

The schematic of the engine used for modeling is shown in Figure 1. The intake and exhaust manifolds are modeled as fixed volumes over which the thermodynamic states remain constant. The fluids are modeled as ideal gases and no heat or mass transfer

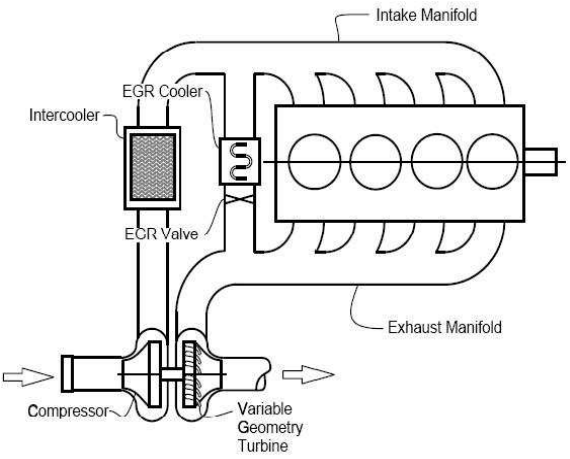

Figure 1. Schematic of the engine ([8])

through the walls is assumed,

$$\frac{dm(t)}{dt} = \dot{m}_{in}(t) - \dot{m}_{out}(t) \tag{1a}$$

$$\frac{dU(t)}{dt} = \dot{H}_{in}(t) - \dot{H}_{out}(t) \tag{1b}$$

where $\dot{m}_i$ and $\dot{H}_i$ represent the mass and enthalpy flow rates. Under these assumptions, the two basic thermodynamic states used in the model are pressure and density (mass). In addition to these, the fraction of burnt gas in the mixture plays an important role in the dynamics and pollutant formation, and must be accounted for. Hence, we have a total of six thermodynamic variables describing the intake and exhaust manifold dynamics. The last state is the turbocharger speed, which is derived from Newton's second law. Thus, the seven-state model is given by,

$$\dot{m}_1 = W_c + W_{egr} - W_e \tag{2a}$$

$$\dot{p}_1 = \frac{c_p R}{c_v V_1}(W_c T_c + W_{egr} T_{egr} - W_{e1} T_1) \tag{2b}$$

$$\dot{F}_1 = \frac{W_{egr}(F_2 - F_1) - W_c F_1}{m_1} \tag{2c}$$

$$\dot{m}_2 = W_e - W_{egr} - W_t + W_f \tag{2d}$$

$$\dot{p}_2 = \frac{c_p R}{c_v V_2}((W_e + W_f) T_e - W_{egr} T_2 - W_t T_2) \tag{2e}$$

$$\dot{F}_2 = \frac{W_e[15.6(1-F_1) + (1+AF)F_1]/(1+AF) - W_e F_2}{m_2} \tag{2f}$$

$$\dot{\omega}_{tc} = \frac{1}{J_{tc}\omega_{tc}}(\eta_m P_t - P_c) \tag{2g}$$

where p_i, F_i, P_i and T_i represent the manifold pressure, fraction of burnt gas, power and temperature. c_p, c_v and R stand for specific heats and gas constant of the mixture. ω_{tc}, J_{tc} and η_m stands for speed, inertia and mechanical efficiency of the turbocharger. W_i represents the mass flow rates, where i stands for 1, 2, c, t and e, which denote the intake manifold, exhaust manifold, compressor, turbine and engine respectively. W_{egr}, W_f and AF represent the mass flow rate through the EGR-valve, the fueling rate and the air-fuel ratio. For details regarding the model, various constants and maps used in generating such a model, the reader is referred to [2], [3], [5], and [6].

This seven-state model is further simplified to a 3-state model for the purpose of controller design. The fractions of burnt gases, F_1 and F_2, are removed as they are difficult to measure and weakly observable from the remaining states. The steady-state value of F_1, which is a performance variable, can be regulated by regulating the AF ratio and EGR flow fraction. The states m_1 and m_2 are also removed, as they are difficult to control independent of p_1 and p_2. Also, the temperatures, T_1 and T_2, are treated as slowly varying external signals and their influence on different gas constants is neglected (see [6] and [5] for details).Thus, we are left with three states. In addition to this, the turbocharger dynamics is modeled as a first-order lag power transfer with time constant τ. Thus, we have the following 3-state model,

$$\dot{p}_1 = k_1(W_c + \tilde{u}_1 - k_e p_1) \tag{3a}$$

$$\dot{p}_2 = k_2(k_e p_1 - \tilde{u}_1 - \tilde{u}_2 + W_f) \tag{3b}$$

$$\dot{P}_c = \frac{1}{\tau}(-P_c + \eta_m k_t (1 - p_2^{-\mu})\tilde{u}_2) \tag{3c}$$

where $\tilde{u}_1$ and $\tilde{u}_2$ represent EGR and VGT flow respectively.

3 Controller Design

3.1 Problem Formulation

In a diesel engine, higher combustion temperature leads to increased NO_x formation. With EGR, this problem can be solved, as the recirculated inert exhaust gas brings down the temperature and thus, reduces the NO_x production. On the other hand, this implies that there is less exhaust gas passing through the VGT, which causes a reduction in boost pressure and power. Hence, there is a trade-off between reduced NO_x formation and power delivered to the compressor and a coordinated approach is required to achieve the twin objectives. These goals can be realized by regulating the air-fuel ratio (AF) and exhaust gas recirculation ratio to certain desired values, based on static engine data. The set points have been found to be functions of engine speed and fueling rate. But, the AFR and EGR ratios are not measured quantities. Hence, these set points are transformed

to the set points for compressor air flow and EGR mass flow, which can then be used to generate the steady-state values for manifold pressures and compressor power. Thus, the control objective is to regulate the states x_1, x_2 and x_3 to zero using u_1 and u_2 as control inputs, where $x_1 = p_1 - \bar{p}_1$, $x_2 = p_2 - \bar{p}_2$, $x_3 = P_c - \bar{P}_c$, $u_1 = \tilde{u}_1 - \bar{u}_1$ and $u_2 = \tilde{u}_2 - \bar{u}_1$. Equation (3) can be written in terms of these new coordinates as,

$$\dot{x_1} = -k_1 k_e x_1 - \varphi_1(x_1) + \psi_1(x_1)x_3 + k_1 u_1 \tag{4a}$$
$$\dot{x_2} = k_2 k_e x_1 - k_2(u_1 + u_2) \tag{4b}$$
$$\dot{x_3} = -\frac{1}{\tau}x_3 + \varphi_2(x_2) + \psi_2(x_2)u_2 \tag{4c}$$

where φ_1, ψ_1, φ_2 and ψ_2 are given by

$$\varphi_1(x_1) = \frac{k_1 k_c \bar{P}_c}{1-\bar{p}_1^{\mu}}\left(\frac{\bar{p}_1^{\mu} - (x_1+\bar{p}_1)^{\mu}}{(x_1+\bar{p}_1)^{\mu} - 1}\right)$$
$$\psi_1(x_1) = \frac{k_1 k_c}{(x_1+\bar{p}_1)^{\mu} - 1}$$
$$\varphi_2(x_2) = \frac{\bar{P}_c}{\tau}\left(\frac{\bar{p}_2^{-\mu} - (x_2+\bar{p}_2)^{-\mu}}{1-\bar{p}_2^{-\mu}}\right)$$
$$\psi_2(x_2) = \frac{\eta_m k_t}{\tau}(1 - (x_2+\bar{p}_2)^{-\mu})$$

Furthermore, in the set $\mathcal{D}$=$\{p_1 > 1, p_2 > 1, P_c > 0\}$,which is the region of interest, the nonlinear functions and their derivatives satisfy the following conditions;

$$\varphi_1(x_1) : x_1\varphi_1(x) > 0$$
$$\frac{\partial \varphi_1}{\partial x_1} > 0 \tag{5a}$$
$$\psi_1(x_1) : \psi_1(x_1) > 0$$
$$\frac{\partial \psi_1}{\partial x_1} < 0 \tag{5b}$$
$$\varphi_2(x_2) : x_2\varphi_2(x_2) > 0 \quad \text{and} \quad -\frac{\bar{P}_c}{\tau} < \varphi_2(x_2) < \frac{\bar{P}_c \bar{p}_2^{\mu}}{\tau(1-\bar{p}_2^{\mu})}$$
$$\frac{\partial \varphi_2}{\partial x_2} > 0 \tag{5c}$$
$$\psi_2(x_2) : 0 < \psi_2(x_2) < \frac{\eta_m k_t}{\tau}$$
$$\frac{\partial \psi_2}{\partial x_2} > 0 \tag{5d}$$

It can be shown that the region $\mathcal{D}$ is invariant ([5]). Furthermore, we will assume that the intake manifold pressures and compressor power are bounded below by a finite value under operating conditions.

3.2 Linear Controller Design

In this section, we study the stability of the origin as an equilibrium point based on Lyapunov's Indirect Method ([11]). We will use the following coordinate transformation, $z_1 = x_3$, $z_2 = x_2$, $z_3 = -Kx_2 - x_1$, $U_1 = u_1 + u_2$, $U_2 = u_2$, where K is an arbitrary scaling constant. The transformation is chosen for two reasons: first, the equilibrium point for the transformed system is unchanged and is given by $z_1 = z_2 = z_3 = 0$; and second, choosing $K = \frac{k_1}{k_2}$ significantly simplifies the equations and the subsequent operations. In these coordinates, equation (4) can be rewritten as,

$$\dot{z}_1 = \frac{-1}{\tau}z_1 + \varphi_2(z_2) + \psi_2(z_2)U_2 \tag{6a}$$
$$\dot{z}_2 = -Kk_2k_e z_2 - k_2 k_e z_3 - k_2 U_1 \tag{6b}$$
$$\dot{z}_3 = Kk_e(Kk_2 - k_1)z_2 + k_e(Kk_2 - k_1)z_3 + \varphi_1(-Kz_2 - z_3) - \psi_1(-Kz_2 - z_3)z_1 + (Kk_2 - k_1)U_1 + k_1 U_2 \tag{6c}$$

With this particular choice of K, the Jacobian $\mathbf{J}$ is given by,

$$\begin{bmatrix} (-\frac{1}{\tau} + \psi_2\frac{\partial U_2}{\partial z_1}) & (\frac{\partial \varphi_2}{\partial z_2} + \psi_2\frac{\partial U_2}{\partial z_2} + U_2\frac{\partial \psi_2}{\partial z_2}) & (\psi_2\frac{\partial U_2}{\partial z_3}) \\ (-k_2\frac{\partial U_1}{\partial z_1}) & (-k_1k_e - k_2\frac{\partial U_1}{\partial z_2}) & (-k_2k_e - k_2\frac{\partial U_1}{\partial z_3}) \\ (-\psi_1 + k_1\frac{\partial U_2}{\partial z_1}) & (\frac{\partial \varphi_1}{\partial z_2} - z_1\frac{\partial \psi_1}{\partial z_2} + k_1\frac{\partial U_2}{\partial z_2}) & (k_1\frac{\partial U_2}{\partial z_3} + \frac{\partial \varphi_1}{\partial z_3} - z_1\frac{\partial \psi_1}{\partial z_3}) \end{bmatrix}$$

The Root-locus and Bode plots for the linearized plant are shown in Figures 2 and 3. It can be concluded from these plots that the uncompensated system is unstable and has nonminimum phase zeros. Now, the task is to stabilize the system using state feedback. This can be achieved by designing a control law that makes the Jacobian matrix Hurwitz. Also, we know that the sum of the diagonal elements is equal to the sum of eigenvalues, which decide the rate of convergence of the states. Hence, it will be to our advantage if can make the trace as large as possible, without rendering the system unstable. Therefore, in view of these design criteria and the Jacobian matrix obtained, we propose the following linear control law,

$$U_1 = C_1 z_2 - k_e z_3 \tag{7a}$$
$$U_2 = -C_2 z_1 - C_3 z_3 \tag{7b}$$

In terms of the original coordinates, the control laws are given by

$$\tilde{u}_1 = C_2 x_3 + (C_1 - \frac{k_1}{k_2}(C_3 - k_e))x_2 - (C_3 - k_e)x_1 + \bar{u}_1 \quad (8a)$$

$$\tilde{u}_2 = -C_2 x_3 + C_3(x_1 + \frac{k_1}{k_2}x_2) + \bar{u}_2 \quad (8b)$$

With this choice of control law, the eigenvalues are given by,

$$\lambda_1 = -(k_1 k_e + k_2 C_1)$$
$$\lambda_2 = -\frac{a}{2} + \frac{\sqrt{a^2 - 4b}}{2}$$
$$\lambda_3 = -\frac{a}{2} - \frac{\sqrt{a^2 - 4b}}{2}$$

where a and b are given by,

$$a = \frac{1}{\tau} + k_1 C_3 + C_2 \psi_{2e} - \frac{\partial \varphi_1}{\partial z_3}\Big|_e$$
$$b = \left(\frac{1}{\tau} + C_2 \psi_{2e}\right)\left(k_1 C_3 - \frac{\partial \varphi_1}{\partial z_3}\Big|_e\right)$$

From equation (5), we know a and b are both positive which implies that this control law indeed makes the Jacobian Matrix Hurwitz. The eigenvalues of the system are directly proportional to the three controller parameters, which can be tuned for getting faster convergence rates.

3.3 Nonlinear Controller Design

3.3.1 Nonlinear Contraction Analysis We begin this section by reproducing the basic theorem and definitions relevant to Nonlinear Contraction Analysis taken from [8].

Definition 1. *For the system $\dot{x} = f(x,t)$, a region of the space is called a contraction region if the Jacobian $\frac{\partial f}{\partial x}$ is uniformly negative definite in that region.*

Theorem 1. *For the system $\dot{x} = f(x,t)$, any trajectory , which starts in a ball of constant radius centered about a given trajectory and contained at all times in a contraction region, remains in that ball and converges exponentially to this trajectory. Moreover, convergence to the given trajectory is guaranteed if the whole state space is a contraction region.*

Therefore, now our task is to design a control law, which will make the Jacobian matrix uniformly negative definite in the region of interest i.e., make $-(J + J^T) > \delta$ in $\mathcal{D}$, where δ is a constant greater than zero.

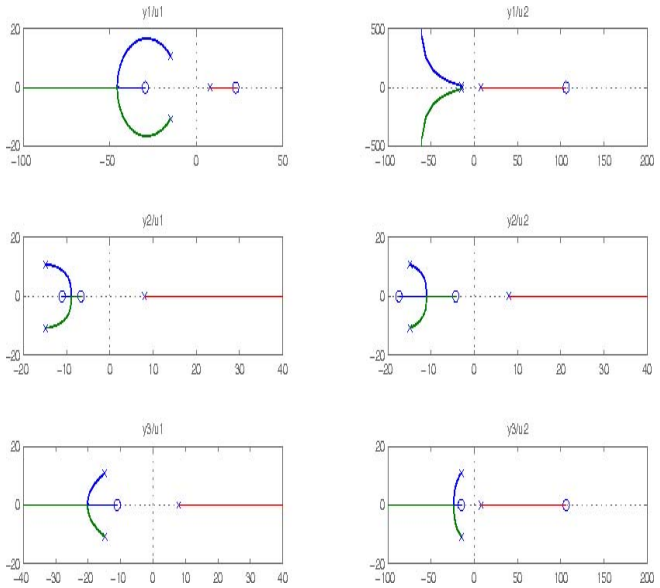

Figure 2. Root-Locus plot of the system

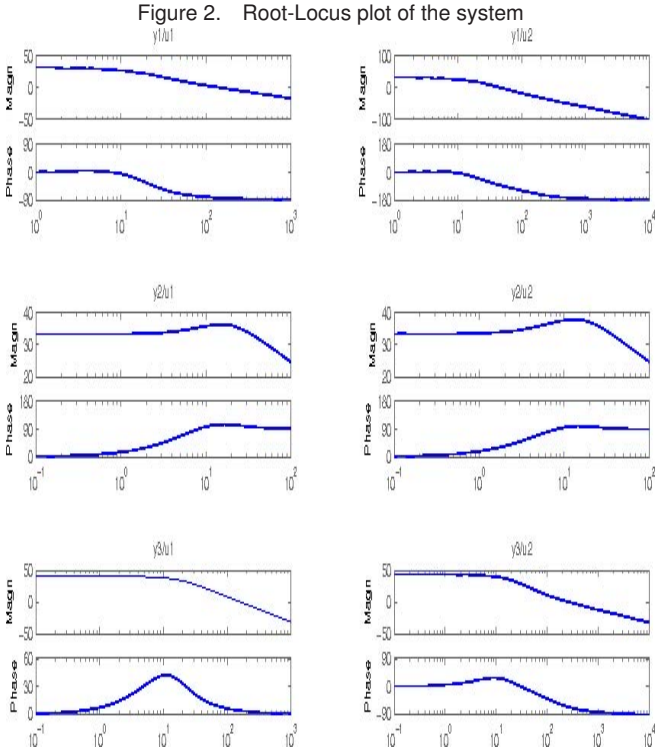

Figure 3. Bode plots of the system

3.3.2 Controller Design The Jacobian matrix J of the system was derived in the previous section. $-(J + J^T)$ is given

by,

$$\begin{bmatrix} a_{11} & a_{12} & a_{13} \\ a_{21} & a_{22} & a_{23} \\ a_{31} & a_{32} & a_{33} \end{bmatrix}$$

where,

$$\begin{aligned}
a_{11} &= 2\left(\frac{1}{\tau} - \psi_2 \frac{\partial U_2}{\partial z_1}\right) \\
a_{12} &= k_2 \frac{\partial U_1}{\partial z_1} - \frac{\partial \varphi_2}{\partial z_2} - \psi_2 \frac{\partial U_2}{\partial z_1} - U_2 \frac{\partial \psi_2}{\partial z_2} \\
a_{13} &= \psi_1 - k_1 \frac{\partial U_2}{\partial z_1} - \psi_2 \frac{\partial U_2}{\partial z_3} \\
a_{22} &= 2\left(k_1 k_e + k_2 \frac{\partial U_1}{\partial z_2}\right) \\
a_{23} &= k_2 k_e + k_2 \frac{\partial U_1}{\partial z_3} - \frac{\partial \varphi_1}{\partial z_2} + z_1 \frac{\partial \psi_1}{\partial z_2} - k_1 \frac{\partial U_2}{\partial z_2} \\
a_{33} &= 2\left(z_1 \frac{\partial \psi_1}{\partial z_3} - k_1 \frac{\partial U_2}{\partial z_3} - \frac{\partial \varphi_1}{\partial z_3}\right)
\end{aligned}$$

and $a_{12} = a_{21}, a_{13} = a_{31}$, and $\quad a_{23} = a_{32}$.
Now, once again we use the same criteria as before but add another condition that the matrix must be positive definite in the entire region of interest. Also, we have to make sure that the nonlinear terms that do not vanish when away from the equilibrium point do not produce a destabilizing effect on the system. In order to achieve these goals, we can modify the linear control law as follows,

$$U_1 = \frac{k_1}{k_2^2}\varphi_1 + C_1 z_2 - k_e z_3 \tag{9a}$$

$$U_2 = \frac{\psi_1}{k_1} z_1 - C_2 z_1 - C_3 z_3 \tag{9b}$$

and in the original coordinates,

$$\begin{aligned}
\tilde{u}_1 = {} & \frac{k_1 \varphi_1}{{k_2}^2} + C_2 x_3 - \frac{\psi_1 x_3}{k_1} + \\
& (C_1 - \frac{k_1}{k_2}(C_3 - k_e))x_2 - (C_3 - k_e)x_1 + \bar{u}_1
\end{aligned} \tag{10a}$$

$$\tilde{u}_2 = -C_2 x_3 + \frac{\psi_1 x_3}{k_1} + C_3(x_1 + \frac{k_1}{k_2} x_2) + \bar{u}_2 \tag{10b}$$

Note that using this control law, we get $a_{23} = a_{32} = 0$. It is known from the theory of linear algebra that if a matrix is positive definite, then the determinants of the upper square left submatrices should be greater than zero. Therefore, in order to show that the Jacobian is negative definite, we have to show that the following two inequalities can always be satisfied by proper choice of gains,

$$\begin{aligned}
& 4\left(\frac{1}{\tau} + C_2\psi_2 - \frac{\psi_1\psi_2}{k_1}\right)\left(k_1 k_e + k_2 C_1 - \left(\frac{k_1}{k_2}\right)^2 \frac{\partial \varphi_1}{\partial z_2}\right) - \\
& \left[\frac{z_1\psi_2}{k_2}\frac{\partial \psi_1}{\partial z_3} - \frac{\partial \varphi_2}{\partial z_2} + (C_2 z_1 - \frac{\psi_1 z_1}{k_1} + C_3 v_3)\frac{\partial \psi_2}{\partial z_2}\right]^2 > 0
\end{aligned} \tag{11}$$

$$\begin{aligned}
& 2\left(k_1 C_3 + \frac{\partial \varphi_1}{\partial z_3}\right)\left[4(\frac{1}{\tau} + C_2\psi_2 - \frac{\psi_1\psi_2}{k_1})\left(k_1 k_e + k_2 C_1 - \left(\frac{k_1}{k_2}\right)^2 \frac{\partial \varphi_1}{\partial z_2}\right)\right. \\
& \left. - \left(\frac{z_1\psi_2}{k_2}\frac{\partial \psi_1}{\partial z_3} - \frac{\partial \varphi_2}{\partial z_2} + (C_2 z_1 - \frac{z_1\psi_1}{k_1} + C_3 v_3)\frac{\partial \psi_2}{\partial z_2}\right)^2\right] - \\
& 2\left(k_1 C_2 + C_3\psi_2 + \frac{z_1\psi_2}{k_1}\frac{\partial \psi_1}{\partial z_3}\right)^2 \left(k_1 k_e + k_1 C_1 - \left(\frac{k_1}{k_2}\right)^2 \frac{\partial \varphi_1}{\partial z_3}\right) > 0
\end{aligned} \tag{12a}$$

$$\begin{aligned}
& \Rightarrow \left[8\left(k_1 C_3 + \frac{\partial \varphi_1}{\partial z_3}\right)4(\frac{1}{\tau} + C_2\psi_2 - \frac{\psi_1\psi_2}{k_1}) - 2\left(k_1 C_2 + C_3\psi_2 + \right.\right. \\
& \left.\left. \frac{z_1\psi_2}{k_1}\frac{\partial \psi_1}{\partial z_3}\right)^2\right]\left(k_1 k_e + k_2 C_1 - \left(\frac{k_1}{k_2}\right)^2 \frac{\partial \varphi_1}{\partial z_2}\right) - 2\left(k_1 C_3 + \frac{\partial \varphi_1}{\partial z_3}\right) \\
& \times \left(\frac{z_1\psi_2}{k_2}\frac{\partial \psi_1}{\partial z_3} - \frac{\partial \varphi_2}{\partial z_2} + (C_2 z_1 - \frac{\psi_1 z_1}{k_1} + C_3 v_3)\frac{\partial \psi_2}{\partial z_2}\right)^2 > 0
\end{aligned} \tag{12b}$$

$$\Rightarrow 2AB - 2CD > 0$$

where,

$$\begin{aligned}
A = {} & \left[8\left(k_1 C_3 + \frac{\partial \varphi_1}{\partial z_3}\right)4(\frac{1}{\tau} + C_2\psi_2 - \frac{\psi_1\psi_2}{k_1})\right. \\
& \left. -2\left(k_1 C_2 + C_3\psi_2 + \frac{z_1\psi_2}{k_1}\frac{\partial \psi_1}{\partial z_3}\right)^2\right] \\
B = {} & \left(k_1 k_e + k_2 C_1 - \left(\frac{k_1}{k_2}\right)^2 \frac{\partial \varphi_1}{\partial z_2}\right) \\
C = {} & 2\left(k_1 C_3 + \frac{\partial \varphi_1}{\partial z_3}\right) \\
D = {} & \left(\frac{z_1\psi_2}{k_2}\frac{\partial \psi_1}{\partial z_3} - \frac{\partial \varphi_2}{\partial z_2} + (C_2 z_1 - \frac{\psi_1 z_1}{k_1} + C_3 v_3)\frac{\partial \psi_2}{\partial z_2}\right)^2
\end{aligned}$$

For A to be greater than zero, it must satisfy the following inequality,

$$8(k_1C_3+\frac{\partial\varphi_1}{\partial z_3})(\frac{1}{\tau}+C_2\psi_2-\frac{\psi_1\psi_2}{k_1})>2(k_1C_2+C_3\psi_2+\frac{z_1\psi_2}{k_1}\frac{\partial\psi_1}{\partial z_3})^2$$

which gives us an inequality in gain C_2 as follows,

$$\Rightarrow -\alpha C_2^2+\beta C_2+\gamma>0 \tag{13}$$

where

$$\begin{aligned}
\alpha &= k_1^2\\
\beta &= 4\psi_2\frac{\partial\varphi_1}{\partial z_3}+2k_1C_3\psi_2-2z_1\psi_2\frac{\partial\psi_1}{\partial z_3}\\
\gamma &= 4(k_1C_3+\frac{\partial\varphi_1}{\partial z_3})(\frac{1}{\tau}-\frac{\psi_1\psi_2}{k_1})-\psi_2^2C_3^2-(\frac{z_1\psi_2}{k_1}\frac{\partial\psi_1}{\partial z_3})^2\\
&\quad -2\frac{z_1\psi_2^2}{k_1}\frac{\partial\psi_1}{\partial z_3}C_3
\end{aligned}$$

Inequality (13) can be satisfied if the discriminant of the quadratic equation is strictly greater than zero i.e., $\beta^2-4\alpha\gamma>0$ for all values of C_2.This gives the following inequality for gain C_3,

$$\left(2k_1C_3\psi_2+4\psi_2\frac{\partial\varphi_1}{\partial z_3}-2z_1\psi_2\frac{\partial\psi_1}{\partial z_3}\right)^2-4k_1^2\left\{\psi_2^2C_3^2+2C_3\frac{z_1\psi_2^2}{k_1}\frac{\partial\psi_1}{\partial z_3}+\left(\frac{z_1\psi_2}{k_1}\frac{\partial\psi_1}{\partial z_3}\right)^2-4\left(k_1C_3+\frac{\partial\varphi_1}{\partial z_3}\right)\left(\frac{1}{\tau}-\frac{\psi_1\psi_2}{k_1}\right)\right\}>0$$

On simplification, we obtain,

$$C_3>-\frac{1}{k_1}\frac{\partial\varphi_1}{\partial z_3} \tag{14}$$

Now, we can choose a value of C_3 that satisfies the above inequality and calculate the value of gain C_2 such that,

$$\frac{\beta}{2\alpha}-\frac{\sqrt{\beta^2+4\alpha\gamma}}{2\alpha}<C_2<\frac{\beta}{2\alpha}+\frac{\sqrt{\beta^2+4\alpha\gamma}}{2\alpha} \tag{15}$$

Most of the expressions in the equations written above are sign definite. In fact, a lower bound for the expressions can be found, as all the states are assumed to be bounded below. Once we have calculated C_2 and C_3 which is within the required bounds, we can use (11) and (12) to calculate a suitable C_1, which will make the right hand side of the equations strictly greater than zero. This guarantees the stability of the system.

4 Results

4.1 Simulation results

In the current work, we evaluate the performance of the controller by implementing it on the 3-state model. Once we obtain more data from the engine, the control laws will be implemented on a more complicated plant. The control objective is to indirectly regulate the AFR and EGR ratios by regulating the compressor flow and EGR flow. Simulations are done using the linear and nonlinear control law derived in the previous section. Figure 4 shows that the response of the system to a step change in fueling from 3 to 6 kg/hr, using the linear control law and Figure 5 shows the variation in control effort. Figure 6 and and Figure 7 are the corresponding plots for nonlinear control law.

4.2 Conclusions

The simulation results indicate the effectiveness of the control laws in stabilizing the system. In fact, the performance of the system can be further improved by properly tuning the three controller parameters. The undershoot and overshoot present in the p_1 tracking profile is due to presence of nonminimum phase zero, as seen in the Root-locus plots. Another point worth mentioning is the effectiveness of the linear control law. Although it appears much simpler to implement, it achieves almost the same level of performance as the nonlinear control laws, at least for the 3-state model. It would be interesting to see how this controller performs in laboratory settings, when compared to the nonlinear controllers.

Most of the controller designs are based on Lyapunov stability analysis. But, when it is difficult to find a Lyapunov function that satisfies all the required conditions, Nonlinear contraction analysis can provide a simple alternate way of doing stability analysis.

Due to inaccuracies in set-point generation, it is possible to have good tracking performance for intermediate variables such as manifold pressures and compressor power, but poor tracking of variables that are actually responsible for pollutant formation. Hence, more accurate methods for set-point generation should be investigated. Also, a better model that uses variables other than those used in this model, e.g. O_2, may lead to more effective controller design.

REFERENCES

[1] Heywood, J., B. (1998). *Internal Combustion Engine Fundamentals*, McGraw-Hill, New York.

[2] Guzzella, L., & Amstutz, A. (1998). Control of diesel engines. *IEEE Transactions on Control Systems Technology, 18(5)*, 54-71.

[3] Guzzella, L., & Onder, C., H. (2005). *Introduction to modeling and control of internal combustion engine systems*, Springer.

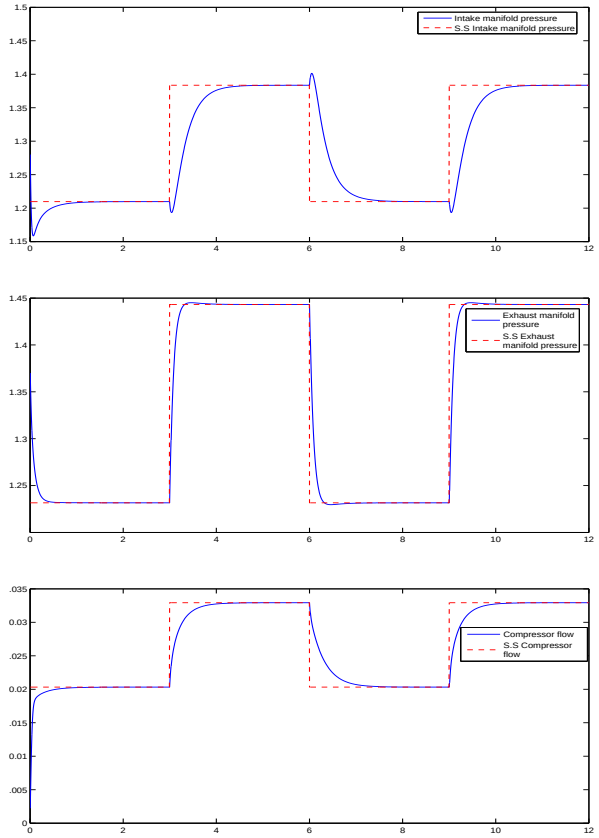

Figure 4. Regulation of manifold pressures and compressor flow using Linear controller

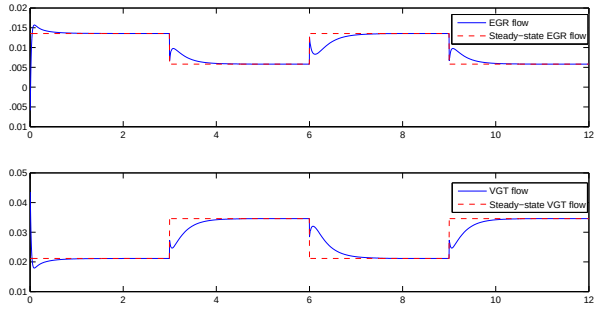

Figure 5. Desired versus actual control effort with Linear controller

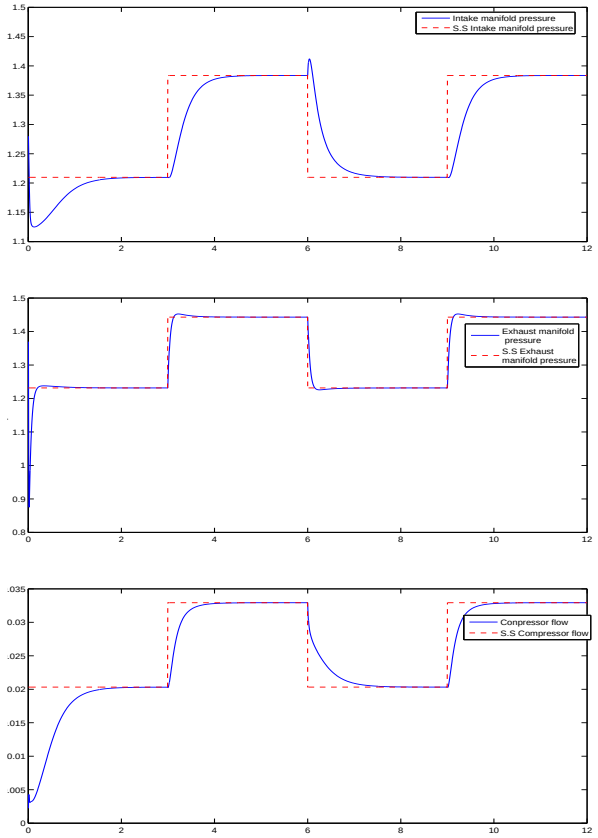

Figure 6. Regulation of manifold pressures and compressor flow using Nonlinear controller

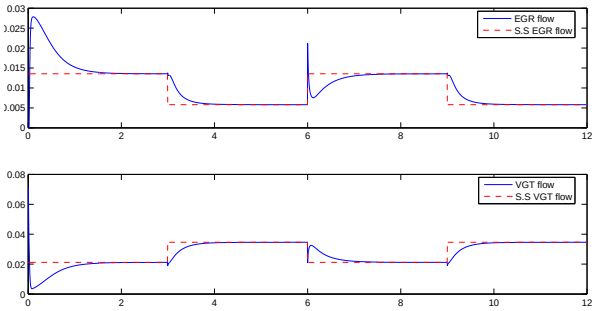

Figure 7. Desired versus actual control effort with Nonlinear controller

[4] Krasovskii, N., N. (1959). *Problems of the Theory of Stability of motion*, Mir, Moscow.

[5] Jankovic, M., Jankovic, M., & Kolmanovsky, I. (2000). Constructive Lyapunov control design for turbocharged diesel engines. *IEEE Transactions on Control Systems Technology, 8(2)*, 288-299.

[6] Kolmanovsky, I., Moraal, P., Nieuwstadt, M., & Stephanopolou, A. (1997). Issues in modeling and control of intake flow in variable geometry turbocharged engines. *Proceedings of the 18th IFIP conference on system modeling and optimization.* Detroit, MI.

[7] Nieuwstadt, M., Moraal, P., Kolmanovsky, I., & Stephanopolou, A.. Decentralized and multivaribale designs for EGR-VGT control of a diesel engine.

[8] Larsen, M., Jankovic, & Kokotovic, P. (2003). Coordinated passivation designs. *Automatica, 39*, 335-341.
[9] Lohmiller, W., & Slotine, J. (1998). On contraction analysis for nonlinear systems. *Automatica, 34(6)*, 683-696.
[10] Stephanopolou, A., Kolmanovsky, I., & Fruedenberg, J. (2000). Control of varibale geometry turbocharged diesel engines for reduced emissions. *IEEE Transactions on Control Systems Technology, 8(4)*, 733-745.
[11] Khalil, H. (2002). *Nonlinear Systems, 3rd ed.,*Prentice Hall, New Jersey.